Hindawi
International Journal of Antennas and Propagation
Volume 2018, Article ID 6878607, 7 pages
https://doi.org/10.1155/2018/6878607

Research Article

Dual-Band Reconfigurable Antenna for Polarization Diversity

Youngje Sung

Electronics Engineering, Kyonggi University, Suwon, Republic of Korea

Correspondence should be addressed to Youngje Sung; yjsung@kgu.ac.kr

Received 20 December 2017; Revised 5 April 2018; Accepted 12 April 2018; Published 26 April 2018

Academic Editor: Ikmo Park

This paper proposes a dual-band reconfigurable square-ring antenna with a polarization diversity property. The proposed antenna consists of a square-ring resonator, two stubs with a shorting via, and two PIN diodes. The stub is positioned symmetrically to the left and right of the square-ring resonator, and the square-ring antenna connected to one of two stubs has a dual-band resonance. In this case, both resonant frequencies exhibit linear polarization (LP), and the two polarized waves are perpendicular to each other. The PIN diode selectively connects only one of the two stubs to the square-ring resonator. Thus, the polarization of the proposed antenna changes electrically at the two resonant frequencies. In addition, the frequency ratio (f_2/f_1) can be easily controlled by changing the length or width of the stub.

1. Introduction

Polarization-reconfigurable antennas have attracted a significant amount of interest due to their advantages, including the elimination of fading losses by multipath effects and frequency bandwidth reuse to increase the channel capacity [1]. To date, numerous studies have been carried out to develop polarization-reconfigurable antenna designs. However, most have been limited to research into polarization diversity between right-handed circular polarization (RHCP) and left-handed circular polarization (LHCP) [2–6]. Furthermore, research into polarization diversity between the orthogonal linear polarizations (LPs) has been relatively inadequate [7–11]. Reference [7] proposed a polarization diversity reconfigurable antenna using a switchable feed structure. When the four PIN diodes were turned on and off independently, the feed point changed, resulting in four different LPs. In [8], four shorting posts and four PIN diodes were placed at a 45° interval, and four PIN diodes controlled the connection between the shorting via and the ground plane. As a result, the antenna can switch between four LPs at 45° intervals. In [9], a reconfigurable slot antenna that switches between the vertical and horizontal LPs was proposed. Two PIN diodes were applied to the CPW-to-slotline transition to control the direction of the electric field that formed in the feed structure. As a result, two LPs perpendicular to each other were realized. In [10], a PIN diode was applied at the end of the feed line. By adjusting the state of the PIN diode, the impedance of the feed end can be electrically switched to be short or open. Thus, the polarization state can be controlled between the two LPs.

To the best of our knowledge, only two studies on polarization diversity between LPs in antennas operating in a dual band have been published. In [12], the authors presented a single-feed dual-band microstrip patch antenna with switchable orthogonal LPs. However, since the frequency ratio was larger than 2 and the difference in the antenna performance at the two resonant frequencies was too large, the proposed antenna can be utilized only in a limited area. In [13], a single-fed dual-band polarization-reconfigurable antenna was first proposed for WLAN applications. The two resonance modes of this antenna, respectively, utilized the TM_{10} and TM_{30} modes of the square-patch antenna. However, since the TM_{30} mode has a higher order, the side lobe was largely generated on a radiation pattern at the second resonant frequency.

In the proposed antenna, the square-ring resonator serves as a radiator and the short-circuit stub, which is placed one on each side, serves to change the polarization of the electric field that forms on the square-ring resonator. To electrically adjust the polarization of the electric field, two PIN diodes are inserted between the square ring and the stub.

Two stubs and two PIN diodes are arranged for the antenna structure to be symmetrical so that the antenna's electrical characteristics remain constant. In this paper, if one of the two stubs is connected to the square ring, the antenna easily exhibits dual-band dual polarization, and in this case, the two LPs are orthogonal to each other [14]. Conversely, if the other stub is connected to the square ring, the polarization at the two resonant frequencies is reversed. The proposed reconfigurable design is implemented and measured, and experimental results on the prototype are also presented and discussed.

2. Antenna Geometry

Figure 1 shows the reconfigurable square-ring antenna proposed in this paper. It exhibits a polarization diversity function in the dual band. Both polarizations are LPs and are perpendicular to each other. The proposed antenna consists of a square-ring resonator that operates as a radiating element, a feed structure, two shorted stubs, and two PIN diodes (HSMP-3864). The proposed antenna is fabricated on a substrate. It is implemented on Rogers RT/duroid 5880™ with a thickness of 1.57 mm, a relative permittivity of 2.2, and a dielectric loss tangent of 0.0009. The length of the one side of the square-ring resonator is denoted by L, and the width of the square ring is denoted by w. Shorted stubs of the length L_s and width w_s are symmetrically placed on the square ring. At this time, two PIN diodes are placed between the square-ring resonator and the stub. Considering the size of the PIN diode, the distance between the radiating ring and the shorting stub is set to 0.5 mm. The width w_f of the feed line is set to 4.8 mm to produce a characteristic impedance of 50 Ω. The PIN diodes have a resistance of 1.5 Ω and a capacitance of 0.2 pF, respectively, in forward bias and reverse bias, respectively. The two PIN diodes operate when 0.75 V is applied and the current consumption is 0.4 mA. A simulation is then performed using the HFSS tool.

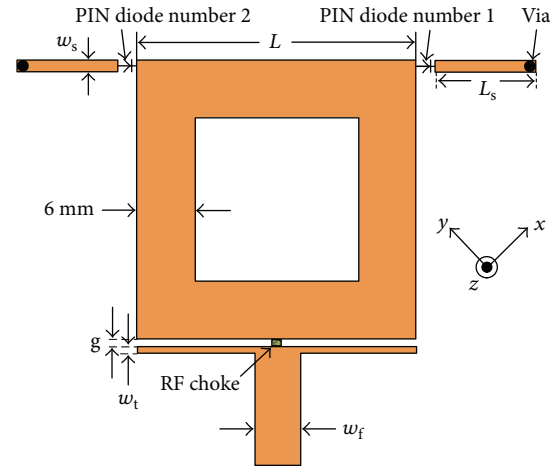

Figure 1: Dual-band reconfigurable antenna with polarization diversity. Dimensions: $L = 26$ mm, $w = 6$ mm, $L_s = 10$ mm, $w_s = 0.5$ mm, $g = 0.8$ mm, $w_t = 0.4$ mm, and $w_f = 4.8$ mm.

3. Polarization of the Square-Ring Antenna with Different Stub Positions

Table 1 shows the simulated E-field distribution for square-ring antennas with different shorted stub positions. The simulation is conducted at two resonant frequencies (f_1 and f_2). The length and width of the stub and the position of the via are all set as equal. In all six modes, the position of the stub is set to 8 mm away from the nearest vertex, and there are eight ways to place the stubs at a distance of 8 mm from the nearest vertex. Since there is a feed structure at the bottom of the square ring, only six total structures are considered. In the simulated results, the electric field is stronger in the dark part and the electric field is weaker in the bright part.

From simulated electric field distributions of the six antennas, we can determine the following important facts. First, regardless of the position of the stub, the electric field distribution that forms on the square-ring resonator at two resonant frequencies always has two nulls. This is consistent with the perimeter of the square-ring antenna corresponding to one wavelength at the resonant frequency. Therefore, the proposed antenna operates in the TM_{11} mode, which is a fundamental mode of the square-ring antenna, at both resonant frequencies. This means that the proposed antenna has a different operating principle from that presented in [13]. Second, even if the position of the stub changes and if the distance from the nearest vertex remains constant, the two resonant frequencies change little. At this time, the square-ring resonator and the feed structure have the same parameters. However, the matching performance at the two resonant frequencies is not constant. In general, the closer to the vertex, the better the matching characteristic at both resonant frequencies [14]. Third, at the first resonant frequency, the weakest electric field on the square-ring antenna is where the stub contacts. Since the end of the stub is shorted through a via, the stub has a very low impedance. Therefore, the impedance for the part connected to the stub becomes low, and the electric field is weak. At the second resonant frequency, the impedance increases at the portion where the stub is located, so a strong electric field forms at this portion as opposed to the first resonant frequency. Most importantly, the electric field distribution at the first resonant frequency and the electric field distribution at the second resonant frequency are orthogonal to each other [14, 15].

There are several associations between the six modes presented in Table 1, and the following are summarized. First, the electric field distributions that appear in mode 1 and mode 6 are the same, and the reason for this is the following. Since the circumference of the square ring corresponds to one wavelength at the corresponding frequency, there are necessarily two electric field null points on the square ring. A stub is definitely connected with one of these two null points. For example, in mode 1, one of the two nulls of the electric field is located on the left side of the square ring, and this is the location where the stub exists. At this time, there is no stub at the other null position of the electric field located on the right side. However, since it is a half wavelength from the null of the left side, naturally, the null of the electric field is formed at this point. In mode 6, the stub is located at the null position on the right side, and the stub

Table 1: Polarization of the square-ring antenna with different stub positions.

	Geometry	f_1	f_2
Mode 1	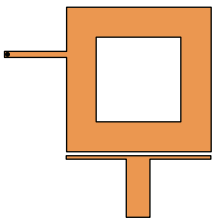	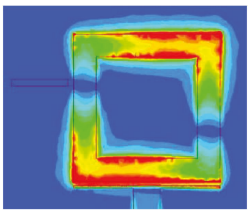	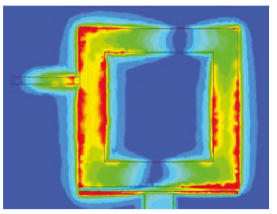
Mode 2	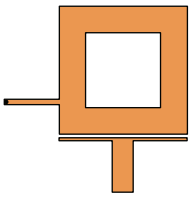	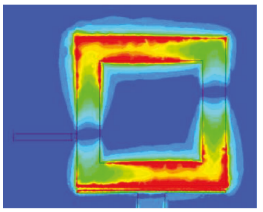	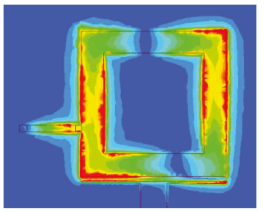
Mode 3	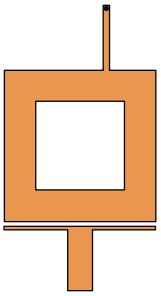	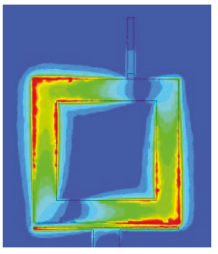	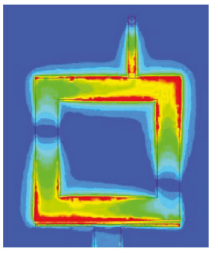
Mode 4	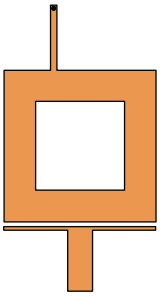	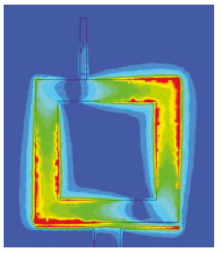	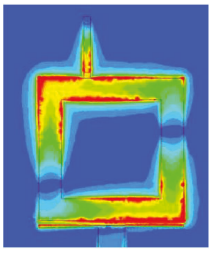
Mode 5	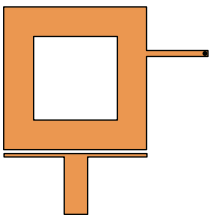	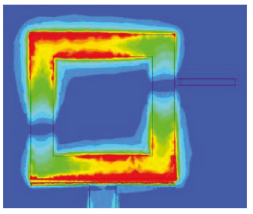	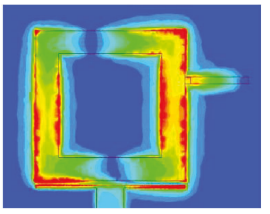
Mode 6	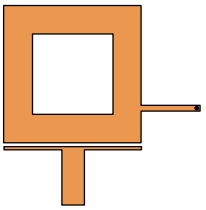	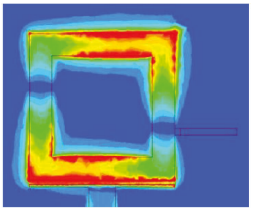	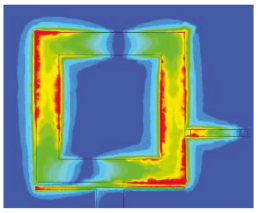

is not present in the null on the left side. Therefore, both modes have the same electric field distribution because they have two electric field null points at the same position. For this reason, modes 2 and 5 have the same electric field distribution. Based on this fact, the electric field distribution formed by the ring antenna does not change when the stub

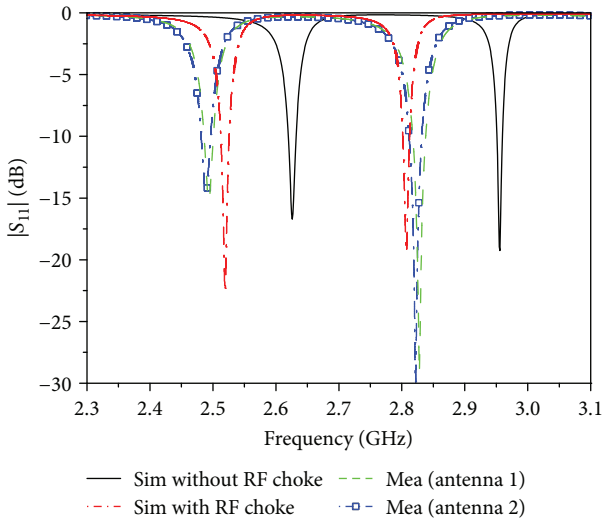

Figure 2: Simulated and measured results of the proposed reconfigurable antenna.

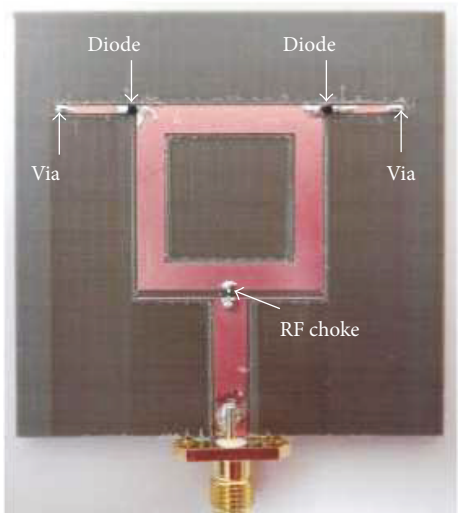

Figure 3: Picture of the fabricated prototype.

is rotated 180° around the center of the square ring. At this time, the two resonant frequencies and matching characteristics of the antenna hardly change.

Second, if the stub position is symmetrical with respect to the square-ring antenna, in modes 1 and 5, modes 2 and 6, and modes 3 and 4, the electric field distribution is also symmetrical at two resonant frequencies. At this time, both resonant frequencies and matching characteristics are also completely the same. Although not shown in Table 1, the stub can be expected to be closer to the vertex, and the polarization of the electric field becomes closer to the diagonal. Based on the above, the electric field distributions of the two antennas are expected to be perpendicular to each other at two resonant frequencies when the two stubs are positioned so as to be in contact with the left-top vertex and the right-top vertex, respectively, and only one of the stubs must be connected to the square ring.

By using such a structure, a reconfigurable antenna with a switchable polarization in a dual band can be realized. As mentioned in [14], as the position of the stub changes, the first resonant frequency does not change, but the second resonant frequency is affected. The reason for this tendency is easily seen from the electric field distribution shown in Table 1. At the first resonant frequency, no electric field is distributed in the stub. Therefore, the first resonant frequency of the square-ring antenna does not change, not only the position of the stub but also the length or width thereof. On the other hand, an electric field can be seen to strongly form in the stub at the second resonant frequency.

4. Dual-Band Polarization-Reconfigurable Antenna

To conveniently measure the operating characteristics of the proposed reconfigurable antenna, a bias voltage is applied to the PIN diode using a bias tee. When a positive voltage is applied to the feed line through the bias tee and a negative voltage is applied to the ground plane, PIN diode number 1 is in the on state and PIN diode number 2 is in the off state. At this time, the right shorted stub is electrically connected to the square-ring antenna. This configuration is referred to as antenna 1. Conversely, if a positive voltage is applied to the ground plane and a negative voltage is applied through the feed section, PIN diode number 1 is in the off state and PIN diode number 2 is in the on state. This configuration is referred to as antenna 2. The shorting pins here act as bias circuits, and the bias network is therefore very simple because there is no need for additional bias lines in this structure. An open stub can be used for the dual-band polarization-reconfigurable antenna implemented in this paper, but a shorted stub is chosen because it is easy to implement the bias structure.

To verify the theoretical analysis mentioned above, the antenna shown in Figure 1 is fabricated and measured. Figure 2 shows the simulated and measured results of the proposed antenna, and the square-ring antenna without an RF choke exhibits a dual resonance ($f_1 = 2.64$ GHz and $f_2 = 2.96$ GHz). At this time, only one of the two stubs is connected to the square-ring antenna, and a 33 nH inductor is used as the RF choke, which is located between the feed structure and the square ring. The simulations show that the two resonant frequencies shift downward by about 100 MHz due to the inductor. Since antennas 1 and 2 are symmetrical, the frequency response is generally the same. The measured 10 dB impedance bandwidth is 42 MHz (2507–2549 MHz) for the lower band and 30 MHz (2795–2825 MHz) for the upper band. The simulation was performed by setting the PIN diode to the equivalent value according to the on/off state. However, since this is not completely accurate, the simulation result is inevitably different from the measurement result. When the length or width of the stub is adjusted, only the second resonant frequency can be adjusted without changing the first resonant frequency, so a dual-band polarization diversity antenna with various

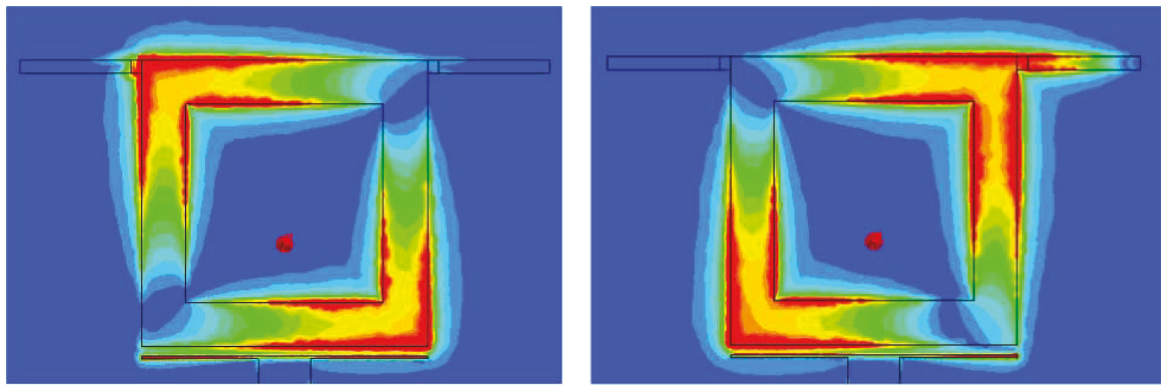

(a) (b)

Figure 4: Simulated E-field distribution of antenna 1: (a) f_1 and (b) f_2.

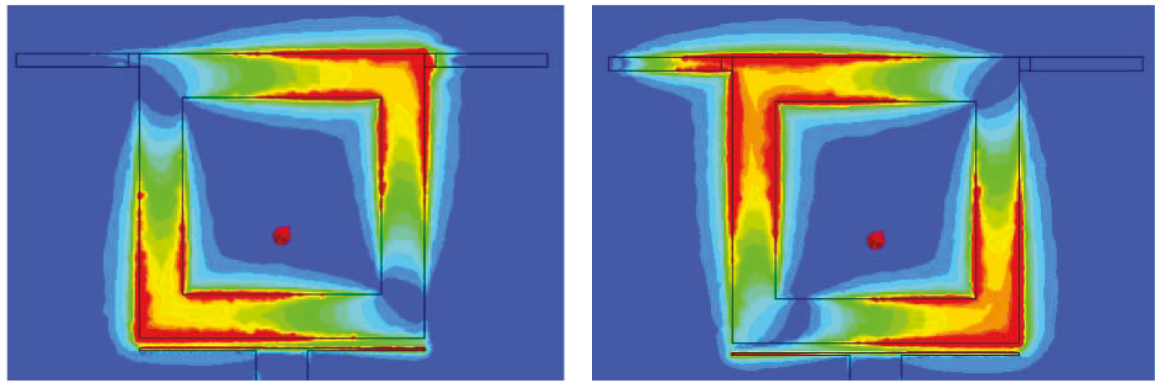

(a) (b)

Figure 5: Simulated E-field distribution of antenna 2: (a) f_1 and (b) f_2.

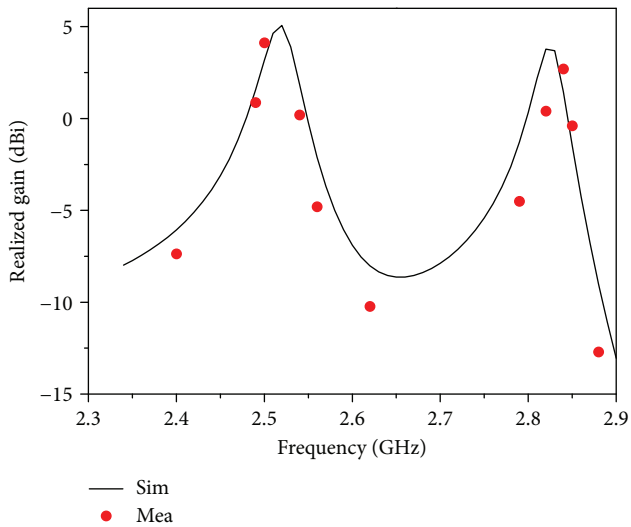

Figure 6: Simulated and measured gain of the proposed reconfigurable antenna.

frequency ratios can be easily realized. The fabricated antenna is shown in Figure 3.

Figures 4 and 5 show the magnitude of the electric field distributed in antennas 1 and 2. The simulation is performed at two resonant frequencies of the antenna. Since antennas 1 and 2 have a symmetrical structure, the two resonant frequencies are the same. As shown in Figure 4(a), at the first resonance frequency, antenna 1 has a null point at the right-top corner because the right stub is connected to the square-ring antenna. As a result, the null line of the electric field forms along the right diagonal line (x direction with respect to the coordinate axis in Figure 1), as described above. That is, the polarization of the electric field forms in the y direction. In the case of antenna 2, since the left stub is connected to a square-ring antenna, the null line of the electric field at the first resonant frequency forms along the left diagonal line (x direction with reference to the coordinate axis in Figure 1). In other words, the polarization of the electric field forms in the x direction. Figures 4(a) and 5(a) show that the two electric field distributions are orthogonal. When the applied voltage is adjusted to change the on/off state of the two diodes, a reconfigurable antenna capable of electrically adjusting two polarizations perpendicular to each other at the first resonance frequency can be realized. In addition, the field distribution at the second resonant frequency appears to be perpendicular to the electric field distribution at the first resonant frequency. Therefore, the proposed structure can be seen to operate as a reconfigurable antenna that can adjust the two polarizations perpendicular to each other, even at the second resonant frequency.

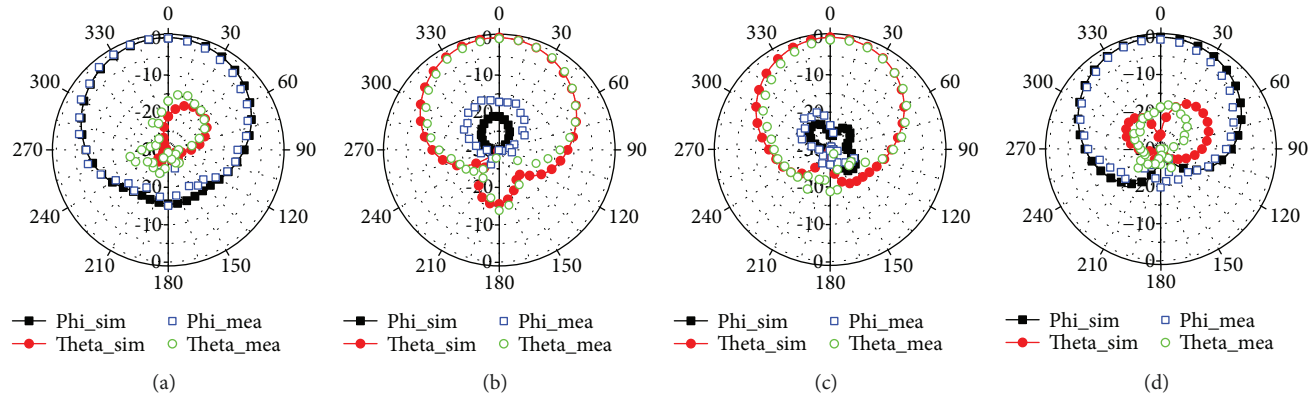

Figure 7: Measured radiation patterns of antenna 1: (a) *yz*-plane at f_1, (b) *xz*-plane at f_1, (c) *yz*-plane at f_2, and (d) *xz*-plane at f_2.

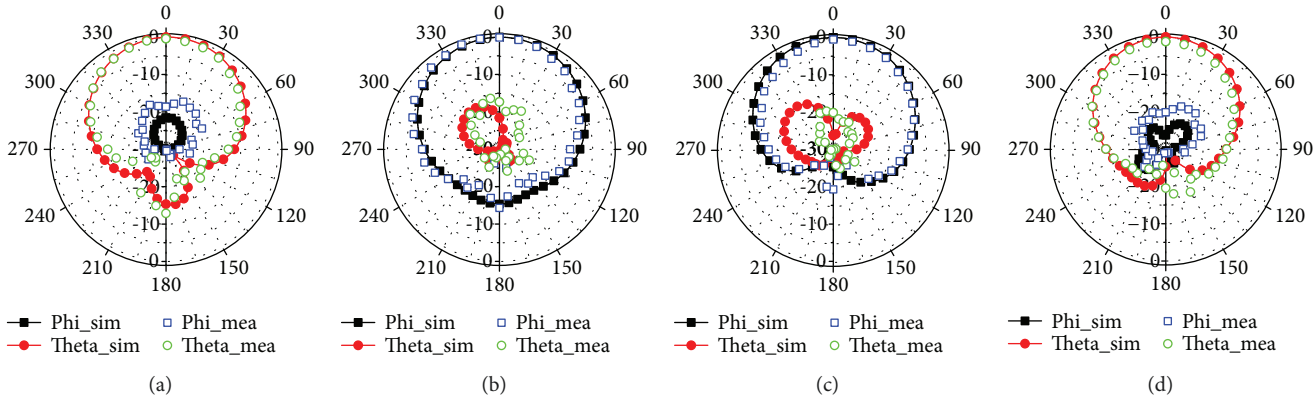

Figure 8: Measured radiation patterns of antenna 2: (a) *yz*-plane at f_1, (b) *xz*-plane at f_1, (c) *yz*-plane at f_2, and (d) *xz*-plane at f_2.

Figure 6 shows the simulated and measured gains with frequency variation. The measured gains of the proposed antenna are 4.12 and 2.81 dBi at two resonant frequencies, respectively. Figures 7 and 8 show the measured radiation patterns for antennas 1 and 2, respectively. In both cases, the radiation pattern is measured at two resonant frequencies of 2.53 and 2.81 GHz. In the radiation pattern, the *E*-plane forms along the plane where the peak E-field is present, while the *H*-plane is determined along the plane including the null of the E-field. For antenna 1, the *E*-plane at the first resonant frequency forms along the *y*-axis. Conversely, it formed along the *x*-axis at the second resonant frequency. For antenna 2, the *E*-plane forms along the *x*- and *y*-axes at two resonant frequencies (f_1 and f_2), respectively. Therefore, the radiation pattern shows that the proposed reconfigurable antenna exhibits polarization diversity between the LPs orthogonal at two resonant frequencies.

5. Conclusion

This paper proposed a dual-band polarization-reconfigurable antenna. A shorted stub is connected to a conventional square-ring antenna to obtain the LP characteristics in the dual band. At this time, the polarization characteristics of the antenna can be easily adjusted by changing the position of the stub. The shorted stubs are located symmetrically to achieve polarization diversity at the same frequency, and the complexity of the structure is reduced by utilizing the shorting pin located at the end of the stub as a bias circuit. The proposed antenna is suitable for wireless communications and mobile satellite communications because of its simple structure.

Conflicts of Interest

The author declares that there is no conflict of interest regarding the publication of this paper.

Acknowledgments

This work was supported by Kyonggi University Research Grant 2016.

References

[1] Y. Wang, F. Zhu, and S. Gao, "Design and investigation of differential-fed ultra-wideband patch antenna with polarization diversity," *International Journal of Antennas and Propagation*, vol. 2016, Article ID 4254830, 6 pages, 2016.

[2] D. Seo and Y. Sung, "Reconfigurable square ring antenna for switchable circular polarisation," *Electronics Letters*, vol. 51, no. 6, pp. 438–440, 2015.

[3] S.-W. Lee and Y. Sung, "Polarization reconfigurable patch antenna with electric current disturbance," *Journal of Electromagnetic Waves and Applications*, vol. 29, no. 16, pp. 2232–2241, 2015.

[4] Y. Huang, J. Geng, X. Liang, R. Jin, and X. Bai, "A novel CP horn antenna with switchable polarization by single port feeding," *International Journal of Antennas and Propagation*, vol. 2015, Article ID 562521, 9 pages, 2015.

[5] W. Li, S. Gao, Y. Cai et al., "Polarization-reconfigurable circularly polarized planar antenna using switchable polarizer," *IEEE Transactions on Antennas and Propagation*, vol. 65, no. 9, pp. 4470–4477, 2017.

[6] S. Karamzadeh, M. Kartal, H. Saygin, and V. Rafii, "Polarisation diversity cavity back reconfigurable array antenna for C-band application," *IET Microwaves, Antennas & Propagation*, vol. 10, no. 9, pp. 955–960, 2016.

[7] H. Gu, J. Wang, L. Ge, and C.-Y.-D. Sim, "A new quadri-polarization reconfigurable circular patch antenna," *IEEE Access*, vol. 4, pp. 4646–4651, 2016.

[8] S.-L. Chen, F. Wei, P.-Y. Qin, Y. J. Guo, and X. Chen, "A multi-linear polarization reconfigurable unidirectional patch antenna," *IEEE Transactions on Antennas and Propagation*, vol. 65, no. 8, pp. 4299–4304, 2017.

[9] Y. Li, Z. Zhang, W. Chen, and Z. Feng, "Polarization reconfigurable slot antenna with a novel compact CPW-to-slotline transition for WLAN application," *IEEE Antennas and Wireless Propagation Letters*, vol. 9, pp. 252–255, 2010.

[10] T. Tokunaga, M. Yamamoto, T. Nojima, and K. Itoh, "Polarisation switchable microstrip array antenna using proximity feeding technique," *Electronics Letters*, vol. 39, no. 22, p. 1569, 2003.

[11] S. W. Lee and Y. Sung, "A polarization diversity patch antenna with a reconfigurable feeding network," *Journal of Electromagnetic Engineering and Science*, vol. 15, no. 2, pp. 115–119, 2015.

[12] F. Meng and S. K. Sharma, "Single feed dual-frequency orthogonal linear- polarization microstrip patch antenna with large frequency ratio," in *2015 IEEE International Symposium on Antennas and Propagation & USNC/URSI National Radio Science Meeting*, pp. 836-837, Vancouver, BC, Canada, July 2015.

[13] P.-Y. Qin, Y. J. Guo, and C. Ding, "A dual-band polarization reconfigurable antenna for WLAN systems," *IEEE Transactions on Antennas and Propagation*, vol. 61, no. 11, pp. 5706–5713, 2013.

[14] Y. Sung, "Stub-loaded square-ring antenna for circular polarization applications," *Journal of Electromagnetic Waves and Applications*, vol. 30, no. 11, pp. 1465–1473, 2016.

[15] S. I. Latif and L. Shafai, "Polarisation and resonant characteristics of gap-loaded microstrip square ring antennas," *IET Microwaves, Antennas & Propagation*, vol. 4, no. 6, p. 733, 2010.